

PACS 78.55.-m, 79.60.-i, 82.80.-d, 82.80.Ms

Chemical composition and light emission properties of Si-rich-SiO_x layers prepared by magnetron sputtering

L. Khomenkova, N. Korsunskaya, M. Sheinkman, T. Stara

*V. Lashkaryov Institute of Semiconductor Physics, National Academy of Sciences of Ukraine
45, prospect Nauky, 03028 Kyiv, Ukraine*

Abstract. The process of thermal decomposition of SiO_x layers prepared by magnetron sputtering is studied with the use of photoluminescence and Auger and SIMS spectroscopies. From these measurements, we obtained the distributions of the emission properties and the chemical composition over the depth. The effect of the redistribution of silicon and oxygen over the depth is found after the high-temperature annealing which results in the formation of a Si nanocrystal. These redistributions result in the appearance of a Si-depleted region near the layer-substrate interface. The formation of a depletion layer is dependent on the excess of Si. A decrease of the silicon content over the depth of annealed layers is accompanied by a decrease of the Si nanocrystal size, as it is evidenced by the blue shift of the photoluminescence maximum. The mechanism of decomposition of SiO_x and the possible reasons for the appearance of a Si-depleted region are discussed.

Keywords: chemical composition, photoluminescence, SiO_x layer, emission properties.

Manuscript received 06.06.07; accepted for publication 19.12.07; published online 31.01.08.

1. Introduction

One of the important tasks of modern optoelectronics is to provide the stable light emission from silicon-based structures. From this point of view, Si particles embedded in the SiO₂ matrix are of great interest. One of the widespread methods of their preparation is the thermal decomposition of nonstoichiometric oxide SiO_x and, in particular, oxide layers prepared by magnetron sputtering.

There is a number of papers devoted to the investigation of the processes responsible for the formation of Si nanoparticles. The dependences of their concentration on the excess silicon content and the substrate temperature were considered, respectively, in [1–3] and [1, 3], the effect of the annealing temperature on the size and the structure of Si inclusions was investigated in [1, 2, 4, 5], and the mechanisms of SiO_x decomposition in the Si and SiO₂ phases were analyzed in [6–10].

However, it was assumed in most papers that the process occurs homogeneously in the whole volume of the layer. Only some authors [6, 11, 12] took into account the possibility of the appearance of an inhomogeneous distribution of Si particles over the depth after high-temperature annealing. Especially, this issue was not addressed to the case of SiO_x layers

prepared by magnetron sputtering. At the same time, the distribution over the depth is of great importance for the comprehension of the process of thermal decomposition of SiO_x layers, as well as for the effective control over and the accurate prediction of the certain characteristics of Si-SiO₂ structures.

In the present paper, we investigate the distributions of the composition and the emission properties of Si-SiO₂ layers prepared by magnetron co-sputtering of Si and SiO₂ by Auger, SIMS, and photoluminescence (PL) spectroscopies over the depth.

2. Experiment

Nonstoichiometric SiO_x films were prepared by radio-frequency magnetron sputtering in the mixed argon-air atmosphere. The partial pressures of argon and air were 0.33 Pa and $2.77 \cdot 10^{-4}$ – $7.86 \cdot 10^{-4}$ Pa, respectively. The sputtering was produced from two separate Si and SiO₂ targets onto a long (15 cm) silicon or quartz substrate. By this method, a change of the volume content of excess Si (C_{Si}) over a wide range was obtained along the layer length.

To estimate C_{Si} in the samples under investigation, a Si layer was deposited using a silicon target only while keeping the deposition conditions to be the same as for the composite layer. C_{Si} was calculated as $C_{Si} = V_{Si}/V_{SiO_x}$,

where V_{Si} and V_{SiO_x} are the volumes (thicknesses) of the layers sputtered from the Si target only and from both targets, respectively, and measured at the corresponding points. The variation of C_{Si} was from 71 % down to 10 %. The average thickness of the deposited layers was about 0.8–1 μm .

To form silicon particles, the samples were annealed for 40 min in a nitrogen atmosphere at a temperature of 1150 °C. The layers were divided then into samples of 0.5 cm in length. As was shown in [13], the photoluminescence (PL) was observed in the annealed samples with C_{Si} in the interval 28–62 %, but the maximum of its intensity was found to be in the range $C_{Si} = 40\text{--}50\%$.

The chemical composition of the layers before and after annealing was determined by Auger and SIMS spectroscopies. Auger spectra were measured by means of a RIBER LAS 2000 spectrometer and recorded in the range of detection energies of 0–1000 eV with a resolution of 3.4 eV. The primary electron beam energy was equal to 3 keV, and the area investigated was $100 \times 100 \mu\text{m}^2$ in the central part of each sample. Step-by-step etching was performed by a 4-keV beam of Ar^+ ions. To calculate the depth distribution of the layer components, it was assumed that the etching speed does not change with the depth. The variation of the intensities of the LMN peaks for “pure” silicon (at 92 eV) and for Si in SiO_2 (at 76 eV) and the KLL peak for oxygen (at 510 eV) was used to evaluate the relative compositions.

The SIMS measurements were carried out by means of a CAMECA IMS 4f mass spectrometer using a 3–14.5-keV Cs^+ primary beam and by negative secondary ion detection. The SIMS spectra were recorded at a primary beam intensity of 50 nA rastering over the central $125 \times 125\text{-}\mu\text{m}^2$ area. The beam blanking mode was used to improve the depth resolution. The dependence of the matrix composition on depth was obtained by measuring the erosion speed and, at the end of each analysis, the depth of the erosion crater by means of a Tencor Alpha Step profilometer with a typical uncertainty of about 1 nm.

PL spectra were excited by the 337-nm line of a nitrogen laser dispersed with an IKS-12 prism spectrometer and detected by a photomultiplier or a Ge detector. To obtain PL spectra as a function of the depth of the layer, a step-by-step etching of the layer in $\text{HNO}_3\text{:HF:CH}_3\text{COOH} = 3\text{:1:16}$ solution was employed. The PL spectra were measured at different temperatures in the range 77–300 K.

3. Results

3.1. Chemical composition of SiO_x layers

Auger spectra were measured only for samples with $C_{Si} > 50\%$ prepared on Si substrates, since a significant decrease of the sample conductivity at lower C_{Si} hampered the performance of these measurements. The intensity profiles of the peaks corresponding to “pure”

Si, Si in SiO_2 , and oxygen for a non-annealed sample with $C_{Si} = 56\%$ are shown in Fig. 1a. It should be noted that these profiles cannot be measured in the top layer of ~ 130 nm in thickness because of its high oxidation. It is seen in the figure that the distributions of Si and O atoms as well as SiO_2 across the layer are homogeneous enough. The concentration of excess Si atoms (“pure” Si peak) was evaluated from the plateau of curve 1 with respect to the total Si content (curves 1 and 3). The total Si content is defined as the sum of the peak intensities for “pure” Si and for Si in SiO_2 . The concentration of excess Si obtained by this way was found to be $\sim 55\%$. This value is in good agreement with C_{Si} calculated from the ratio of volumes of sputtered Si and SiO_x .

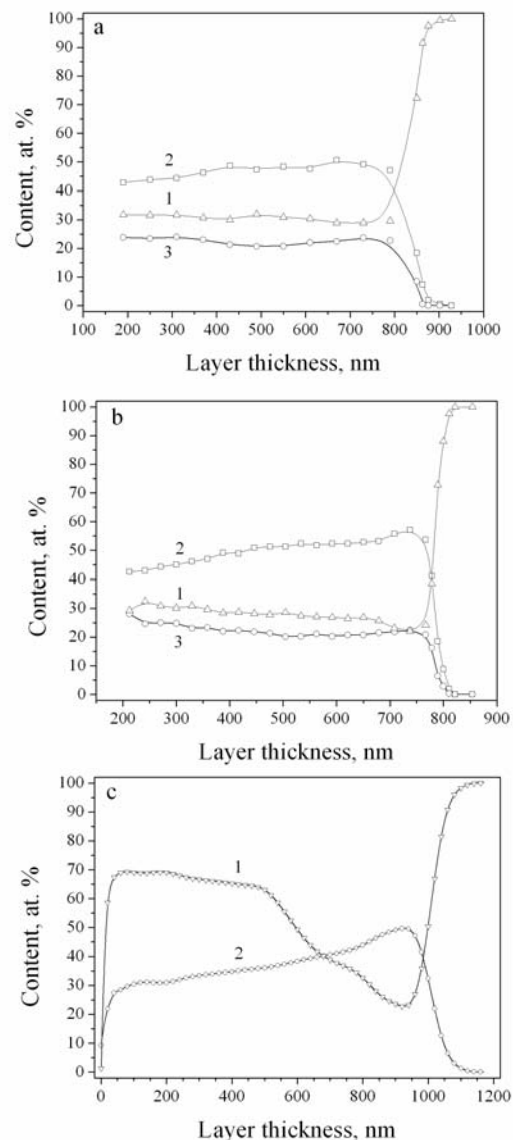


Fig. 1. Depth profiles of “pure” silicon (curve 1), oxygen (2), and SiO_2 (3) before (a) and after annealing at 1150 °C (b) for a sample with $C_{Si} = 56\%$ and (c) the depth distribution of the total silicon (curve 1) and oxygen (2) contents in a sample with $C_{Si} = 68\%$. The results were obtained by Auger spectroscopy.

After annealing, a redistribution of silicon and oxygen is observed across the layer (from the surface to the interface with the substrate). There is a decrease of the silicon content and an increase of oxygen, which results in a Si-depleted and O-enriched region near the substrate (Fig. 1b). The effect is more pronounced in samples with higher excess Si content. This can be seen from Fig. 1c, where the depth distributions of oxygen and the total Si content in the sample with $C_{Si} = 68\%$ are presented.

SIMS studies were performed on samples prepared both on silicon and quartz substrates. They show a homogeneous enough distribution of silicon and oxygen in non-annealed samples while, in annealed samples, they confirm the presence of a Si depleted region near the layer-substrate interface for samples on both types of substrates. This is true for samples with $C_{Si} \geq 40\%$. When C_{Si} decreases, the depleted region diffuses at first and then disappears (at $C_{Si} < 30\%$). Therefore, this Si-depleted region is observed only for $C_{Si} = 40-68\%$ (Fig. 2a, b).

It should be noted that, besides the Si depleted region, a small increase of the Si content is observed in the depth of a layer on the quartz substrate (Fig. 2b, curve 1). The comparison of Si and oxygen depth distributions in this sample (not shown here) indicates that this increase is due to the substrate and is obviously a result of the incorporation of sputtered Si atoms.

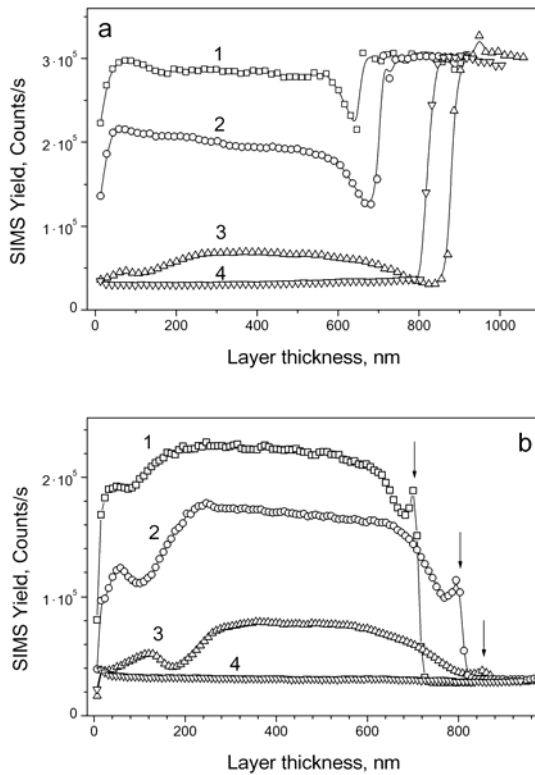


Fig. 2. SIMS profiles of the Si content in layers sputtered on silicon (a) and quartz (b) substrates under identical conditions. Curves 1-4 (in both figures) correspond to C_{Si} values: 1 – 68, 2 – 55, 3 – 41, 4 – 28 %.

An inhomogeneity of the Si distribution for samples with $C_{Si} > 40\%$ was observed also in the subsurface region. In some of them, the Si content in this region decreases, while it has a more complicated behavior in others. The latter is found mainly in samples on quartz substrates (Fig. 2b).

The depth distribution of oxygen demonstrates, as a rule, an increase of the oxygen content near the substrate regions independently of the type of substrate (not shown). In addition, in the case of Si substrates, a small narrow peak was found close to the substrate. This peak can be attributed to the incorporation of sputtered oxygen atoms in the substrate, similar to the peak of the Si content observed in samples prepared on quartz substrates. We note that an increase of the oxygen content in the near-surface region was also found in some samples prepared on quartz substrates.

3.2. Photoluminescence spectra

Before annealing the samples, no photoluminescence was observed. After annealing, the PL spectra contained one PL band. The position of the maximum is shifted to higher energies with decrease in the Si content [14]. The changes of the PL intensity and its peak position under layer-by-layer etching for a sample prepared on a Si substrate are shown in Fig. 3. The value of C_{Si} in this sample was 53 % and is close to the silicon content of the sample, whose composition profile is presented in Fig. 1. We see in Fig. 3 that the PL intensity under layer-by-layer etching is at first constant and then decreases. Simultaneously, as PL decreases, there is a gradual blue shift of the PL peak position from 1.35 to 1.54 eV. The PL peak position shows also a red shift with increase in temperature, in accordance with the Si bandgap shrinkage.

In the case of quartz substrates, the distribution of the PL intensity is more inhomogeneous. However, in this case, the PL intensity also decreases near the substrate and a blue shift of the peak position is observed (not shown).

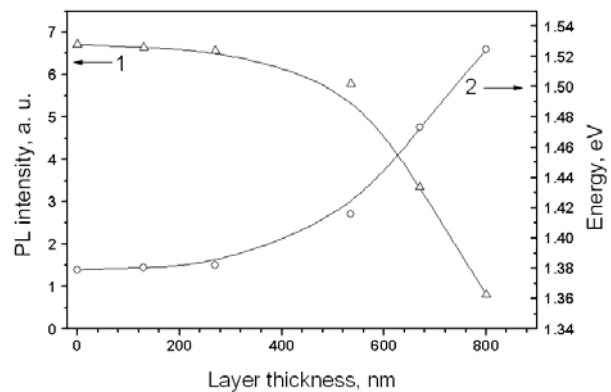


Fig. 3. Dependences of the PL intensity (curve 1) and its peak position (2) on the thickness of the scored layer for a sample with $C_{Si} = 53\%$.

4. Discussion

The as-deposited samples consist of a mixture of the amorphous phases of Si and SiO₂. The annealing at 1150 °C leads to the formation of Si crystallites in the SiO₂ matrix. This is evidenced by the appearance of intense photoluminescence. Indeed, the shift of the PL peak position to higher energies with the decrease of Si content, as well as its red shift with increase in temperature in accordance to the Si band gap shrinkage, are typical of PL bands caused by the exciton recombination in Si crystallites.

The data presented show that the depth distributions of Si and O atoms in the as-sputtered samples are sufficiently homogeneous. However, the process of SiO_x decomposition is accompanied by the appearance of the inhomogeneity of the layer composition over the depth in samples with higher C_{Si} (C_{Si} > 40 %), namely, by the formation of a region which is Si-depleted and oxygen-enriched near the substrate.

Generally, a Si-depleted region could be formed by diffusion of Si atoms to the substrate. Such a possibility was considered in [6]. It was assumed that the Si/SiO₂ interface is a sink for these atoms and, as a result, a Si-depleted region is formed. If this is the case, such a region should appear only in the samples on Si substrates. However, in our case, the Si-depleted region was observed also for samples sputtered on quartz substrates. Another argument against this assumption is the absence of Si accumulation near the layer-substrate interface in the case of the quartz substrate. Thus, we can conclude that the Si redistribution is a result of the Si diffusion towards the surface, while oxygen moves towards the layer/substrate interface.

It can be assumed that the Si and SiO₂ phase separation during the SiO_x decomposition leads not only to the formation of Si inclusions in the SiO₂ matrix, but also to the appearance of a Si-depleted layer near the substrate. Under such an assumption, the smearing of the Si-depleted region and its disappearance with decrease in the excess Si content can be explained by the competition of two processes: the formation of Si inclusions and the Si diffusion to the surface.

In the samples with high Si content, the spinodal mechanism of SiO_x decomposition has to be expected [6, 9, 10, 15]. In this case, the decomposition is determined by the migration of oxygen [16] and proceeds by the rapid initial segregation forming a phase of Si and a SiO₂ shell (that can be considered as nuclei) and a slow growth of the amorphous Si phase due to diffusion processes within these nuclei [9, 10]. The density of nuclei depends on the annealing temperature and can be insufficient to involve all the excess Si in the formation of Si inclusions in our samples. In such a case, the Si diffusion to the surface can be noticeable. At a low Si content, the mechanism of random nucleation, growth, and Ostwald ripening of Si precipitates that is determined by the diffusion of Si can give the contribution to the decomposition process. In this case,

the whole excess Si can be expected to form Si inclusions.

Our results show that, in spite of the fact that oxygen diffusion is predicted to determine the process of SiO_x spinodal decomposition, the diffusion of silicon can also be important.

The diffusion processes that result in the redistribution of silicon and oxygen affect also the PL characteristics of Si/SiO₂ layers, as well as the sizes and the concentrations of crystallites.

Let us consider the changes of the PL characteristics with depth and their correlation with layer composition. Our measurements of the light transmission by the samples on quartz substrates show that, in the samples with C_{Si} > 50 %, the absorption factor of the exciting light (337 nm) is $k \geq 10^5 \text{ cm}^{-1}$. This means that the thickness of the excited region is significantly less than the initial Si-SiO₂ layer thickness d ($kd \gg 1$). It is obvious that, in the region in which this inequality is valid, the changes of the PL intensity and its peak position under layer-by-layer etching reflect the depth distribution of the PL characteristics. However, the inequality $kd \gg 1$ will be eventually violated during etching due to a decrease of both the layer thickness and the “pure” Si content.

As for the samples sputtered on Si substrates, the “pure” Si concentration changes insignificantly in most parts of the layer, and the PL intensity and the PL band peak position are nearly constant in the region of ~250 nm in thickness. Therefore, we can conclude that, in this region, the inequality $kd \gg 1$ is valid, and the concentration of emitting centers is constant. The further decrease of the PL intensity can be caused by the violation of the inequality $kd \gg 1$. Because the PL peak position shows a red shift with temperature in accordance to the Si bandgap shrinkage before and after etching to different thicknesses of the layer, the PL band can be ascribed to the exciton recombination. In this case, the observed uniform depth distribution of the PL intensity and the constant PL peak position imply a homogeneous distribution of the concentrations and the sizes of Si crystallites, while the shift of the PL band peak position to the high-energy side in the deeper part of the sample testifies to a decrease in the size of crystallites. This is in agreement with a decrease of the concentration of “pure” Si and an increase of the concentration of SiO₂.

In the case of the samples on quartz substrates, the behavior of the PL characteristics is more complex. The reason for their nonmonotonous changes is not clear so far and requires further investigations.

5. Conclusions

We have studied the process of thermal transformation of SiO_x layers prepared by magnetron sputtering. It is shown that the high-temperature annealing results in the formation of Si crystallites in the SiO₂ matrix and causes also the appearance of a Si depleted region near the

layer-substrate interface. With decrease in the excess Si content, this depleted region smears at first and then disappears. This is explained by the competition of two processes: the formation of Si inclusions in the SiO₂ matrix and the diffusion of Si atoms in the direction of the surface. It is found that a decrease of the silicon content in the depth of annealed layers is followed by a decrease of the sizes of particles, which is accompanied, in turn, by a shift of the photoluminescence maximum to higher energies.

Acknowledgements

This work was supported by the National Academy of Sciences of Ukraine. The authors thank C. Sada and E. Trave (University of Padua, Italy) for the help in the SIMS measurements and Y. Goldstein, J. Jedrzejewski, and E. Savir (Hebrew University, Israel) for providing the samples.

References

1. L. You, C.L. Heng, S.Y. Ma, Z.C. Ma, W.H. Zong, Z. Wu and G.G. Qin // *J. Cryst. Growth* **212**, p. 109 (2000).
2. H. Seifarth, R. Grotzschel, A. Markwitz, W. Matz, P. Nitzsche, and L. Rebohle // *Thin Solid Films* **330**, p. 202 (1998).
3. S. Charvet, R. Madelon, and R. Rizk // *Solid-State Electronics* **45**, p. 1505 (2001).
4. L.A. Nesbit // *Appl. Phys. Lett.* **46**, p. 38 (1985).
5. L.X. Yi, J. Heitmann, R. Scholz, and M. Zacharias // *J. Phys.: Condens. Matter* **15**, S2887 (2003).
6. T. Muller, K.-H. Heinig, and W. Moller // *Appl. Phys. Lett.* **81**, p. 3049 (2002).
7. A. Lan, B. Liu, and X. Bai // *Jpn J. Appl. Phys. Part 2*, **36**, L1019 (1997).
8. T. Inokuma, Y. Wakayama, T. Muramoto, R. Aoki, Y. Kurata, and S. Hasegana // *J. Appl. Phys.* **83**, p. 2228 (1998).
9. B.J. Hinds, F. Wang, D.M. Wolfe, C.L. Hinkle, and G. Lucovsky // *J. Non-Cryst. Sol.* **227-230**, p. 507 (1998).
10. B.J. Hinds, F. Wang, D.M. Wolfe, C.L. Hinkle, and G. Lucovsky // *J. Vac. Sci. Technol. B* **16**, 2171 (1998).
11. Y. Maeda // *Phys. Rev. B* **51**, p. 1658 (1995).
12. C. Spinella, C. Bongiorno, G. Nicotra, E. Rimini, A. Muscara, and S. Coffa // *Appl. Phys. Lett.* **87**, 044102 (2005).
13. L. Khomenkova, N. Korsunska, V. Yukhimchuk, B. Jumayev, T. Torchunska, A. Vivas Hernandez, A. Many, Y. Goldstein, E. Savir and J. Jedrzejewski // *J. Lumin.* **102-103**, p. 705 (2003).
14. M. Baran, L. Khomenkova, N. Korsunska, T. Stara, M. Sheinkman, Y. Goldstein, J. Jedrzejewski, and E. Savir // *J. Appl. Phys.* **98**, 113515 (2005).
15. M.S. Dunaevskii, J.J. Grob, A.G. Zabrodskii, R. Laiho, A.N. Titkov // *Semiconductors* **38**, p. 1254 (2004).
16. V.A. Dan'ko, I.Z. Indutnyy, V.S. Lysenko, I.Yu. Maidanchuk, V.I. Min'ko, A.N. Nazarov, A.S. Tkachenko, P.E. Shepeliavyi // *Semiconductors* **39**, 1197 (2005).